

Distributed Deep Convolutional Neural Networks for the Internet-of-Things

Simone Disabato
Politecnico di Milano
Milano, Italy
simone.disabato@polimi.it

Manuel Roveri
Politecnico di Milano
Milano, Italy
manuel.roveri@polimi.it

Cesare Alippi*
Politecnico di Milano
Milano, Italy
cesare.alippi@polimi.it

ABSTRACT

Due to the high demand in computation and memory, deep learning solutions are mostly restricted to high-performance computing units, e.g., those present in servers, Cloud, and computing centers. In pervasive systems, e.g., those involving Internet-of-Things (IoT) technological solutions, this would require the transmission of acquired data from IoT sensors to the computing platform and wait for its output. This solution might become infeasible when remote connectivity is either unavailable or limited in bandwidth. Moreover, it introduces uncertainty in the “data production to decision making”-latency, which, in turn, might impair control loop stability if the response should be used to drive IoT actuators.

In order to support a real-time recall phase directly at the IoT level, deep learning solutions must be completely rethought having in mind the constraints on memory and computation characterizing IoT units. In this paper we focus on Convolutional Neural Networks (CNNs), a specific deep learning solution for image and video classification, and introduce a methodology aiming at distributing their computation onto the units of the IoT system. We formalize such a methodology as an optimization problem where the latency between the data-gathering phase and the subsequent decision-making one is minimized. The methodology supports multiple IoT sources of data as well as multiple CNNs in execution on the same IoT system, making it a general-purpose distributed computing platform for CNN-based applications demanding autonomy, low decision-latency, and high Quality-of-Service.

CCS CONCEPTS

•Computing methodologies → Machine learning;
•Computer systems organization → Sensor networks;
Embedded software;

KEYWORDS

Embedded Systems, Deep Learning, Convolutional Neural Networks, Approximate Computing.

1 INTRODUCTION

Deep learning represents the state-of-the-art in many recognition/classification applications [14]. Differently from traditional “shallow” solutions, where features are designed manually, deep learning solutions learn both the most appropriate feature representation and the classification/recognition/prediction task [6] directly from available data. To achieve this goal, deep learning solutions are organized into a pipeline of processing layers to which an increasing granularity of the representation is associated. For

this reason such solutions are typically characterized by a high computational load and memory occupation¹.

Due to such high resource demands, the recall phase of such architectures is mostly restricted to high performance computing units, e.g., those in servers, Cloud or computing centers. In pervasive systems, like those involving the Internet-of-Things (IoT), the recall phase requires the transmission of acquired data from the sensors (e.g., cameras for image/video or microphones for acoustic processing) to the Cloud for neural processing. Unfortunately, this request might become infeasible if the “data production to decision making”-latency at the IoT units does not match with real-time constraints, e.g., those needed to provide a prompt intervention. The system stability might even be compromised when a remote connectivity between IoT units and Cloud is unavailable or limited in bandwidth. It follows that applications requesting a (quasi) real time decision/actuation cannot take advantage of a remote Cloud-based processing of deep learning solutions.

To address these issues deep-learning processing solutions should be moved as close as possible to the place where data are gathered. This would permit the designer to make IoT systems autonomous (decisions are taken locally) and able to minimize the “data production to decision making”-latency as well as reduce the required communication bandwidth [4]. Unfortunately, being embedded systems, IoT units are constrained by computation, memory and, not rarely, energy. That said, in order to support deep neural processing in IoT systems, the design of deep learning solutions must be completely rethought by taking into account hardware and physical constraints at application design-time. As an example, consider the scenario of video-surveillance in Smart Cities, where a system of IoT units equipped with cameras is deployed in a specific location where particular security/safety decisions have to be taken very quickly (despite the possible limited or intermittent available bandwidth).

To match the complexity of deep learning solutions with the constraints of IoT units we exploit the hierarchical processing characterizing deep learning solutions to suitably place the layers of this processing on the IoT units. More specifically, this paper aims at enabling the deep learning recall phase on IoT systems by introducing a methodology for the optimal placement of the layers of the deep learning solutions to IoT units. In particular, given the proven effectiveness of Convolutional Neural Networks (CNNs) to process images and videos (they represent the state-of-the-art

¹For example, the AlexNet Convolutional Neural Network encompasses approximately 61 million parameters requiring more than 230 MB for the storage of the network weights only and more than 725 million floating-point operations to provide an output; the VGG-16 Convolutional Neural Network is even more demanding in terms of memory and computation, i.e., more than 138 million parameters requiring more than 527 MB for the storage and more than 13 billion operations to process the input image.

*Cesare Alippi is also with Università della Svizzera Italiana, Switzerland.

[18]) and the huge memory and execution load required, this paper focuses on CNNs for image recognition/classification applications running in IoT systems. The proposed methodology receives in input both CNNs (whose processing and classification layers have been previously trained) and the technological constraints describing the IoT units and provides as output the optimal placement of the CNN layers to the IoT units minimizing the "data production to decision making"-latency, hence minimizing the time from data gathering to decision. Following the transfer learning approach [23], the deployed CNN can be easily reconfigured to address a different image-classification problem by replacing the classification layers (e.g., see [11]). IoT network reconfiguration (e.g., removal or addition of IoT units) is addressed by periodically executing the placement procedure.

The methodology is general enough to be applied both to traditional CNNs where the processing pipeline, defined at design-time, sequentially operates by processing all the layers up to the final classification one, such as in the Alexnet [18], ResNet [13], or Yolo [19] architectures, and to CNNs where the processing path is built at execution-time according to the information content of the input, such as in Gate-Classification CNNs [11]. Moreover, the Gate-Classification CNN architecture is particularly suitable for IoT systems since the computational load is tunable through a user-defined parameter. In addition, the proposed methodology can be used with CNNs sharing processing layers following the transfer learning approach [23].

All in all, the novel contents of the paper are:

- A methodology for the optimal placement of CNNs in IoT systems minimizing the latency in decision making, measured as the sum of transmission and processing times;
- The methodology can be applied both to CNNs where the processing pipeline is defined at design-time and CNNs where the processing load depends on the information content brought by the input;
- The methodology is tailored to three specific configurations: single CNN, single CNN with Gate-Classification, and multiple CNNs without and with shared processing layers.

The proposed methodology has been validated considering state-of-the-art CNNs and off-the-shelf IoT devices. The provided solutions cover a large class of applications, e.g., those associated with image/video/signal processing (e.g., video analytics for public safety or control of critical sites, smart areas within Industry 4.0, smart cities).

The paper is organized as follows. Section 2 analyses the related literature, while the research problem is formulated in Section 3. The proposed methodology is described in Section 4, while Section 5 presents three relevant configurations. Experimental results are detailed in Section 6, while conclusions are drawn in Section 7.

2 RELATED LITERATURE

The problem of reducing the complexity of deep learning solutions so as to match the technological constraints of IoT systems can be addressed at different levels.

At the hardware level, such a problem could be addressed by designing ad-hoc computing platforms for deep learning based on

custom hardware (e.g., FPGA). This family of solutions could lead to distributed computing units characterized by better technological performance and less power consumption than general-purpose off-the-shelf embedded computing platforms. Unfortunately, these advantages come at the expense of a complex design phase requiring high skills and expertise as well as lack of flexibility in updating the deep learning solutions running on the distributed units [8].

The reduction of complexity of deep learning solutions could be achieved by considering approximation techniques, such as quantization, coding or weight compression[5][10][12]. Several works exist in this field providing meaningful reduction in memory occupation but with a negligible effect on the reduction of computational load. In this path, [11] introduces task-dropping and precision-scaling mechanisms to design application-specific and approximated CNNs able to be executed in off-the-shelf embedded systems. Unfortunately, this methodology does not encompass the possibility to design deep learning solutions able to operate in a distributed system of IoT units.

A different point of view is provided by the off-loading techniques for distributed computing systems. Here, the goal is not to reduce the complexity of deep learning solutions but to move computationally-intensive processing to the high-performing units of the distributed system. For example, a framework to optimally offload code to computing units in a pervasive system is proposed in [20]. There, the goal is to minimize either the total communication latency or the overall energy consumption by relying on a directed acyclic graph modelling the computation of the distributed application and taking into account the connectivity issues characterizing mobile devices. Similarly, in [7] the code is offloaded to more powerful computing units to reduce energy consumption. The goal is to manage the unreliability of wireless communications by considering code checkpoints and common portions of code to be re-used to restart the computation when the communication fails. Differently, [15] proposes a high-level programming language to design applications to be run on Fog-Computing Sensor Networks able to hide the heterogeneity of computing nodes and their position in the space. Very few works present in the literature encompass the code-offloading of machine learning-based applications in pervasive systems. For example, in [9] the classification/pattern recognition tasks of the machine learning-based application running on a wearable device are partially offloaded to other computing units (e.g., mobile phones) according to a graph characterizing the distances among the units. Similarly to our vision, here the priority in the offloading is to move code at first to the closest mobile devices and, then, if needed, to the Cloud. In [2] a distributed Fog-based architecture is used to support the reinforcement learning task in a multi-agent domain. This solution relies on a compiler that defines at design time the mechanisms and the code to be off-loaded from pervasive devices to the Fog. Unfortunately, to be effective, these solutions require powerful enough computing units to support the off-loading of the code, an assumption that rarely holds in the considered IoT technological scenario.

The problem of distributing deep learning solutions has been recently addressed also in the field of edge and fog computing. For example, [21] introduces a distributed framework for multi-view CNNs operating in edge computing platforms. Despite not introducing solutions to deploy the CNN over the pervasive units, this work

shares some affinities with the Gate-Classification mechanisms [11] by considering thresholds on the classifier confidence to skip part of the CNN computation.

We emphasize that the idea of distributing the processing of deep learning solutions in IoT systems proposed in this paper shares some affinities with the in-network distributed processing in wireless sensor networks. Unfortunately, these solutions, e.g., [17], encompass only very simplistic types of processing (i.e., averaging or filtering), making these solutions infeasible for deep learning processing. To the best of our knowledge, the problem of distributing the deep learning processing on different (and potentially heterogeneous) IoT units has never been explored so far in the literature.

3 PROBLEM FORMULATION

The pervasive system is composed by a set of data-generating units $\{s_1, \dots, s_C\}$ acquiring the images to be classified by the C CNNs, a set $\mathbb{N}_N = \{1, \dots, N\}$ of N (possibly heterogeneous) IoT units for computation and the target unit f that is the recipient of the decisions made by the C CNNs. Without any loss of generality, the C data-generating units are assumed to only acquire the data and thus do not participate to the computation. The i -th IoT unit $i \in \mathbb{N}_N$ is characterized by specific constraints on maximum memory usage \bar{m}_i and tolerated computation load \bar{c}_i .

Let d_{i_1, i_2} , for each $i_1, i_2 \in V = \{\mathbb{N}_N \cup \{s_1, \dots, s_C, f\}\}$, be the *hop-distance* between units i_1 and i_2 of V defined as the number of intermediate units, i.e., the number of hops, data need to pass through to connect units i_1 and i_2 . In other terms, the distance d_{i_1, i_2} is the length of the shortest path between units i_1 and i_2 within the graph $G(V, E)$ of nodes in V and arcs in E . An arc e_{i_1, i_2} among units i_1 and i_2 exists in E if i_2 is within the range of the transmission technology the IoT unit i_1 is equipped with². Following the definition of shortest path in a graph, if no path between two units i_1 and i_2 exists, then $d_{i_1, i_2} = +\infty$. Furthermore, we also assume that no isolated nodes exist, i.e., $d_{i_1, i_2} < \infty$, for each $i_1, i_2 \in V$.

Without any loss in generality, we assume that the number of CNNs to be optimally placed on the IoT system is C , i.e., one CNN for each source. Let M_u , for each $u \in \mathbb{N}_C = \{1, \dots, C\}$, be the number of layers characterizing the u -th CNN, i.e., the number of subsequent tasks that have to be executed to classify an input image. Each layer j of CNN u , for each $j \in \{1, \dots, M_u\}$ and $u \in \mathbb{N}_C$, is characterized by a given demand on memory $m_{u,j}$ and computation $c_{u,j}$. More specifically, the memory complexity $m_{u,j}$ (in Bytes) is defined as the number of weights that layer j of CNN u has to store multiplied by the size of the data type used to represent those parameters (typically the floating point type occupying 4 Bytes), while the computational load $c_{u,j}$ of layer j of CNN u is measured as the number of multiplications to be executed by that layer as suggested in [3]. In addition, let $K_{u,j}$, for each $u \in \mathbb{N}_C$ and $j \in \{1, \dots, M_u\}$, be the memory occupation of the intermediate representation transmitted from layer j to the subsequent layer $j+1$ of CNN u , and

²In this paper all the units in V are assumed to share the same transmission technology with a fixed transmission data-rate. Please note that if two nodes adopt different technologies, the proposed definition does no longer represent a distance since it might not be symmetric. In fact, if the IoT units i_1 and i_2 adopts two different transmission technologies such that i_2 is within the transmission range of i_1 , but i_1 is not inside the one of i_2 , then $d_{i_1, i_2} = 1 \neq d_{i_2, i_1}$.

$K_{u,s}$ and K_{u,M_u} be the memory occupation of the input image of CNN u transmitted from the u -th source s_u to the unit executing first layer of the u -th CNN and of the final classification (provided by layer M_u) sent to recipient f , respectively. In particular, K_{u,M_u} could be either the classification label or the posterior probability of the classes.

Examples of memory $m_{u,j}$ and computational $c_{u,j}$ demands, and memory occupations $K_{u,j}$ of CNNs are given in Section 6.1.

When the processing path of the CNNs depends on the information content, such as in Gate-Classification CNNs [11], the decision about the input is made as soon as enough confidence about the classification is achieved (hence skipping the execution of the remaining layers). To achieve this goal, such networks are endowed with intermediate exit points, called *Gate-Classification layers*, which create multiple paths within the CNNs each of which is characterized by a probability of being traversed. More formally, given a M_u -layer Gate-Classification CNN, let $p_{u,j} \in [0, 1]$ be the probability that the j -th layer of the u -th CNN processes the input image and let $g_{u,j} \in [0, 1]$, for each $u \in \mathbb{N}_C$ and $j \in \{1, \dots, M_u\}$, be the probability that the computation ends at layer j of the u -th CNN going directly to f computed as

$$g_{u,j} = \begin{cases} p_{u,j} - p_{u,j+1} & j < M_u \\ 1 - \sum_{v=1}^{M_u-1} g_{u,v} & j = M_u \end{cases}$$

The probabilities $p_{u,j}$ s are estimated during the learning of the Gate-Classification CNN as explained in [11].

We emphasize that, thanks to the transfer learning paradigm [23], the hierarchy of layers of the CNNs can be considered as feature extractors and the image-classification application implemented by the IoT system can be reconfigured by simply updating the final classification layers of the CNNs or the Gate-Classification layers of Gate-Classification CNNs.

The problem we want to address in this paper is the optimal placement of the processing layers of the C CNNs on the N IoT units to minimize the latency in making decisions about the images gathered by the C sources.

4 THE PROPOSED METHODOLOGY

This section introduces the proposed methodology for the optimal placement of the CNNs processing on the IoT system. Such a methodology has been reformulated as an optimization problem aiming at assigning the layers of the C CNNs to the N IoT units minimizing the latency in making a decision. We emphasize that this optimization phase can be periodically executed to manage variations in the IoT network configuration (e.g., removal or insertion of IoT units).

The proposed methodology relies on the *CNM* variables $\alpha_{u,i,j}$ defined as follows:

$$\alpha_{u,i,j} = \begin{cases} 1 & \text{if IoT unit } i \text{ executes the layer } j \text{ of CNN } u \\ 0 & \text{otherwise} \end{cases} \quad (1)$$

for each $u \in \mathbb{N}_C$, for each $i \in \mathbb{N}_N$ and for each $j \in \mathbb{N}_M = \{1, \dots, M\}$, being $M = \max\{M_1, \dots, M_u\}$ the maximum number of layers among the considered C CNNs (i.e., the maximum depth of all the CNNs).

Without loss of generality, the distances d_{i_1, i_2} , for each $i_1, i_2 \in V$, can be precomputed, allowing us to define an integer quadratic optimization problem on the variables $\alpha_{u, i, j}$. As detailed in Section 3, both the sources $\{s_1, \dots, s_C\}$ and f do not participate to the optimization since they are only meant to acquire the images and receive the classification. This assumption can be easily removed by considering additional IoT computing units in the same positions of s_i s and f .

The objective function models the latency in making a decision by the C CNNs distributed to the IoT system, defined as the time between images of size $K_{u, s}$ are gathered by s_u and the corresponding decision K_{u, M_u} is transmitted to f . Hence, the objective function to be minimized becomes:

$$\sum_{u=1}^C \sum_{i=1}^N \sum_{k=i}^N \sum_{j=1}^{M-1} \alpha_{u, i, j} \cdot \alpha_{u, k, j+1} \cdot p_{u, j+1} \cdot \frac{K_{u, j}}{\rho} \cdot d_{i, k} + \sum_{i=1}^N t_i^{(p)} + t_s + t_f \quad (2)$$

with constraints

$$\forall i \in \mathbb{N}_N \quad \sum_{u=1}^C \sum_{j=1}^M \alpha_{u, i, j} \leq L \quad (3)$$

$$\forall i \in \mathbb{N}_N \quad \sum_{u=1}^C \sum_{j=1}^M \alpha_{u, i, j} \cdot m_{u, j} \leq \bar{m}_i \quad (4)$$

$$\forall i \in \mathbb{N}_N \quad \sum_{u=1}^C \sum_{j=1}^M \alpha_{u, i, j} \cdot c_{u, j} \leq \bar{c}_i \quad (5)$$

$$\forall u \in \mathbb{N}_C, \forall j \in \mathbb{N}_M \quad \sum_{i=1}^N \alpha_{u, i, j} = \begin{cases} 1 & \text{if } j \leq M_u \\ 0 & \text{otherwise} \end{cases} \quad (6)$$

and where

$$t_s = \sum_{u=1}^C \sum_{i=1}^N \alpha_{u, i, 1} \cdot p_{u, 1} \cdot \frac{K_{u, s}}{\rho} \cdot d_{s, i} \quad (7)$$

$$t_i^{(p)} = \sum_{u=1}^C \sum_{j=1}^M \alpha_{u, i, j} \cdot p_{u, j} \cdot \frac{c_{u, j}}{e_i} \quad (8)$$

$$t_f = \sum_{u=1}^C \sum_{i=1}^N \sum_{j=1}^M \alpha_{u, i, j} \cdot g_{u, j} \cdot \frac{K_{u, M_u}}{\rho} \cdot d_{i, f} \quad (9)$$

The objective function in Eq. (2) comprises four different components of the latency:

(i) The source time t_s , defined in Eq. (7), required to transmit the images from the sources s_u s to the IoT units executing the first layer of the CNNs. We emphasize that, despite the first layer is always reached i.e., $p_{u, 1} = 1$ for each $u \in \mathbb{N}_C$, the term $p_{u, 1}$ has been inserted in Eq. (7) to provide the homogeneity in the problem formalization.

(ii) The transmission time of the intermediate representations among the IoT units processing the CNN layers. More formally, the transmission time of the intermediate representation of the j -th layer of the u -th CNN from unit i to k is

$$\frac{K_{u, j}}{\rho} \cdot d_{i, k} \quad (10)$$

where ρ is the data-rate of the considered transmission technology and $d_{i, k}$ is the hop-distance between unit i and k as defined in Section 3. In Eq. 2 the transmission time is weighted by the probability $p_{u, j+1}$ that layer $j+1$ is executed right after layer j .

(iii) The processing time of the CNN layers on the IoT units. More specifically, the processing time $t_i^{(p)}$ of the layer j of the CNN u on the i -th IoT unit is approximated as the ratio between the computational demand $c_{u, j}$ that layer requires and the number of multiplications e_i the IoT unit i is able to carry out in one second³. In Eq. (8), the processing time is weighted by the probability $p_{u, j}$ that the layer j of CNN u is executed.

(iv) The sink time t_f required to transmit the final decision K_{u, M_u} , for each $u \in \mathbb{N}_C$, from the IoT units taking these decisions to the sink f . It is noteworthy to point out that Eq. (9) takes into account all the feasible output paths from a node i to the sink f , suitably weighted by the probability $g_{u, j}$ that the classification is made at layer j of CNN u placed on IoT unit i .

The constraint in Eq. (3) ensures that each IoT unit contains at most L layers, being L an additional user-defined model parameter. In particular, when $L = 1$, at most one layer can be assigned to a given IoT unit, while $L > 1$ implies that more layers (also belonging to different CNNs) can be assigned to an IoT unit. The constraints in Eq. (4) and (5) are meant to take into account the technological constraints on memory usage and computational load characterizing each unit. Finally, the constraint in Eq. (6) ensures that each layer j , for each $j \in \mathbb{N}_M$, is assigned to exactly one node and, at the same time, deals with the possibility that the C CNNs might be characterized by a different number $M_u \leq M$ of layers, for each $u \in \mathbb{N}_C$. In fact, in those cases in which $M_u < M$, the unneeded $\alpha_{u, i, j}$ s are set to 0.

When the layer j_1 -th layer of CNN u_1 and the layer j_2 -th of CNN u_2 are shared between the two CNNs, the following constraint is added to the optimization problem

$$\forall i \in \mathbb{N}_N \quad \alpha_{u_1, i, j_1} = \alpha_{u_2, i, j_2} \quad (11)$$

to ensure that the shared layer is placed on the same IoT unit. The constraints on the maximum number of layers placed on a IoT unit - Eq. (3) - and the memory usage and computational load constraints - Eqs (4) and (5) - are modified to count the shared layer only once, as follows:

$$\forall i \in \mathbb{N}_N \quad \sum_{u=1}^C \sum_{j=1}^M \alpha_{u, i, j} \leq L + \alpha_{u_2, i, j_2} \quad (12)$$

$$\forall i \in \mathbb{N}_N \quad \sum_{u=1}^C \sum_{j=1}^M \alpha_{u, i, j} \cdot m_{u, j} \leq \bar{m}_i + \alpha_{u_2, i, j_2} \cdot m_{u_2, j_2} \quad (13)$$

$$\forall i \in \mathbb{N}_N \quad \sum_{u=1}^C \sum_{j=1}^M \alpha_{u, i, j} \cdot c_{u, j} \leq \bar{c}_i + \alpha_{u_2, i, j_2} \cdot c_{u_2, j_2} \quad (14)$$

If a layer is shared among k CNNs, the change proposed in Eqs. (12), (13), and (14) needs to take into account $k - 1$ out of the k variables corresponding to the shared layer.

³The e_i s encompasses the number of available cores, the type of pipeline such cores implement to approach one operation per clock cycle, the (potential) presence of a GPU that allows to parallelize most of the CNN operations (e.g., the convolutions) and all the delays resulting from the management of the processing system and the memory.

The outcome of the optimization problem is the optimal placement $\alpha_{u,i,j}$ s of the layers of the C CNNs to the N IoT units minimizing the delay in making a decision. In the event that the optimization problem provides more than one solution, the optimal assignment of the CNNs to the pervasive system is any solution with minimal latency⁴.

It is crucial to point out that the considered class of optimization problems, i.e., the integer quadratic programs, is NP-complete. More specifically, since the variables are only binary, it is possible to convert it to a integer linear program, and, by relaxing the equality constraint in Eq. 6 as a greater or equal one, our problem becomes one of the Karp's 21 NP-complete problems [16]. Here, we rely on a solver to find the optimal solution of the proposed optimization problem, thus no specific algorithm is defined at this time.

5 TAILORING THE METHODOLOGY TO THREE SPECIFIC CNN CONFIGURATIONS

The general methodology described in the previous section is here tailored to three specific configurations of CNNs. Section 5.1 introduces the case where a single CNN is considered, whereas Section 5.2 tailors the methodology to the case where one Gate-Classification CNN is taken into account. Finally, Section 5.3 describes the model for the case of multiple CNNs running in the same IoT system with and without shared processing layers.

5.1 The configuration with a single CNN

When the number of CNNs is equal to one, i.e., $C = 1$, the formalization in Eq. (1) simplifies in NM binary variables $\alpha_{i,j}$, to determine whether layer j of the CNN is assigned to unit i of the IoT system or not:

$$\alpha_{i,j} = \begin{cases} 1 & \text{if IoT unit } i \text{ executes layer } j \text{ of the CNN} \\ 0 & \text{otherwise} \end{cases}$$

for each $i \in \mathbb{N}_N$ and $j \in \mathbb{N}_M$. The objective function in Eq. (2) modelling the latency in making a decision to be minimized is reformulated as:

$$\sum_{i=1}^N \sum_{k=i}^N \sum_{j=1}^{M-1} \alpha_{i,j} \cdot \alpha_{k,j+1} \cdot \frac{K_j}{\rho} \cdot d_{i,k} + \sum_{i=1}^N t_i^{(p)} + t_s + t_f \quad (15)$$

The constraints in Eq. (3), (4), (5) and (6) are reformulated as

$$\forall i \in \mathbb{N}_N \quad \sum_{j=1}^M \alpha_{i,j} \leq L \quad (16)$$

$$\forall i \in \mathbb{N}_N \quad \sum_{j=1}^M \alpha_{i,j} \cdot m_j \leq \bar{m}_i \quad (17)$$

$$\forall i \in \mathbb{N}_N \quad \sum_{j=1}^M \alpha_{i,j} \cdot c_j \leq \bar{c}_i \quad (18)$$

$$\forall j \in \mathbb{N}_M \quad \sum_{i=1}^N \alpha_{i,j} = 1 \quad (19)$$

⁴More advanced mechanisms could be considered, e.g., selecting the configuration characterized by the lowest energy consumption in transmission or computation.

while

$$t_s = \sum_{i=1}^N \alpha_{i,1} \cdot \frac{K_s}{\rho} \cdot d_{s,i} \quad (20)$$

$$t_i^{(p)} = \sum_{j=1}^M \alpha_{i,j} \cdot \frac{c_j}{e_i} \quad (21)$$

$$t_f = \sum_{i=1}^N \alpha_{i,M} \cdot \frac{K_M}{\rho} \cdot d_{i,f} \quad (22)$$

account for the transmission time between the source s and the IoT unit running the first layer of the CNN, the processing time on the unit i , and the transmission time between the unit running the M -th layer of the CNN and the sink f , respectively.

As an example, the methodology has been applied to:

- the CNN described in Figure 1a, characterized by $M = 5$ layers and whose memory demand m_j s, computational load c_j s, and size of the intermediate representation K_j s are detailed in Section 6.1 - Table 1;
- the pervasive system described in Figure 1b, comprising $N = 11$ IoT units and with s and f sharing the same technological unit. The IoT units belong to two different technological families: STM32H7 (round nodes) and Odroid-C2 (squared nodes). The memory \bar{m}_i and computational \bar{c}_i constraints of these two families of IoT units are detailed in Table 3.

An example of the outcome of the optimization problem in this scenario with $L = 1$ is depicted in Figure 1c, whose corresponding $\alpha_{i,j}$ s are detailed in Figure 1d. The optimal placement comprises the STM32H7 unit n_{05} executing layer $L1$, the Odroid-C2 units n_{10} and n_{04} executing layers $L2$ and $L3$, respectively, and finally STM32H7 units n_{01} and n_{06} executing layers $L4$ and $L5$, respectively. As expected, the layer $L3$ of the CNN has been assigned to an Odroid-C2 IoT unit (i.e., n_{04}) since its execution on STM32H7 would violate the memory constraint.

5.2 The configuration with a single Gate-Classification CNN

This configuration refers to the case where a single Gate-Classification CNN has to be placed on the IoT system.

Here, the $p_{u,j}$ s and $g_{u,j}$ s are simplified as p_j and g_j , for each $j \in \mathbb{N}_M$, defining the probability the layer j is executed and that the final classification is made at layer j (i.e., the direct path from j to the sink is traversed), respectively.

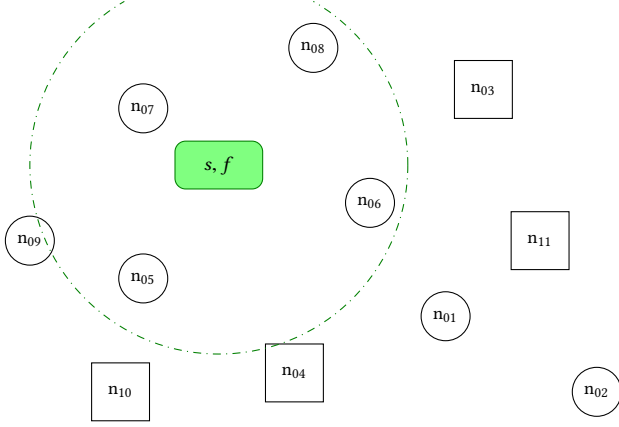
The objective function modelling the latency in decision making defined in Eq (2) is here tailored to a single Gate-Classification CNN:

$$\sum_{i=1}^N \sum_{k=i}^N \sum_{j=1}^{M-1} \alpha_{i,j} \cdot \alpha_{k,j+1} \cdot p_{j+1} \cdot \frac{K_j}{\rho} \cdot d_{i,k} + \sum_{i=1}^N t_i^{(p)} + t_s + t_f \quad (23)$$

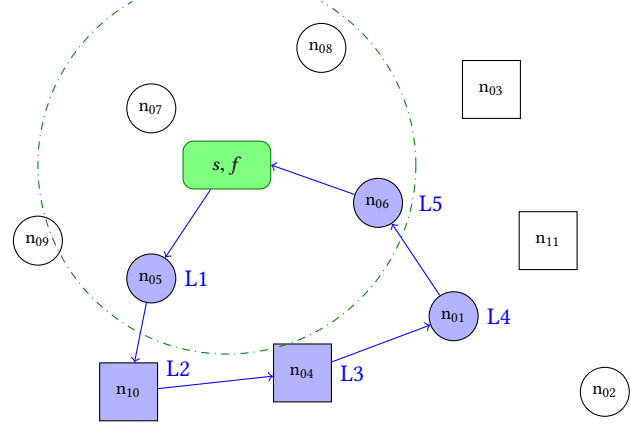
with constraints as in Eqs. (16), (17), (18), and (19), and where the source time t_s , the processing time $t_i^{(p)}$ and the sink time t_f have



(a) The architecture of the considered 5-layer CNN, where I is the input image. The kind of layers are convolutional, maximum pooling or fully-connected.



(b) An example of IoT system. The units with rounded border are STM32H7, while the squared ones are Odroid-C2. The source s and the sink f share the same IoT unit. The dotted circle refers to the transmission range, equal for all the IoT units and here depicted only for the IoT unit with s and f .



(c) The outcome of the methodology where the layers L1, ..., L5 of the 5-layer CNN in Figure 1a are placed on the IoT units of the system shown in Figure 1b, with setting $L = 1$.

	n01	n02	n03	n04	n05	n06	n07	n08	n09	n10	n11
L1	0	0	0	0	1	0	0	0	0	0	0
L2	0	0	0	0	0	0	0	0	0	1	0
L3	0	0	0	1	0	0	0	0	0	0	0
L4	1	0	0	0	0	0	0	0	0	0	0
L5	0	0	0	0	0	1	0	0	0	0	0

(d) The variables $\alpha_{i,j}$ s representing the outcome of the methodology for the solution shown in Figure 1c.

Figure 1: Single-CNN configuration. The methodology is applied to the 5-layer CNN shown in Figure 1a on the IoT system detailed in Figure 1b.

been modified as follows:

$$t_s = \sum_{i=1}^N \alpha_{i,1} \cdot p_1 \cdot \frac{K_s}{\rho} \cdot d_{s,i} \quad (24)$$

$$t_i^{(p)} = \sum_{j=1}^M \alpha_{i,j} \cdot p_j \cdot \frac{c_j}{e_i} \quad (25)$$

$$t_f = \sum_{i=1}^N \sum_{j=1}^M \alpha_{i,j} \cdot g_j \cdot \frac{K_M}{\rho} \cdot d_{i,f} \quad (26)$$

A 6-layer Gate-Classification CNN is shown, as an example, in Figure 2a and detailed in Table 1, where $M = 6$ and the Gate-Classification is at layer $j = 2$. Here, the probability that the classification is made at the Gate-Classification layer, thus skipping the execution of Layers 3 to 6, is $v = 0.99$ (please refer to [11] for details). For this reason, $p_1 = p_2 = 1$ and $p_3 = p_4 = p_5 = 0.01$. Moreover, Figure 2a shows also the values of g_j s of the 6-layer Gate-Classification CNN, being different from zero only at the Gate-Classifier ($j = 2$) and at the last layer ($j = 6$). In Figure 2, the proposed methodology is applied to this CNN and the IoT system already

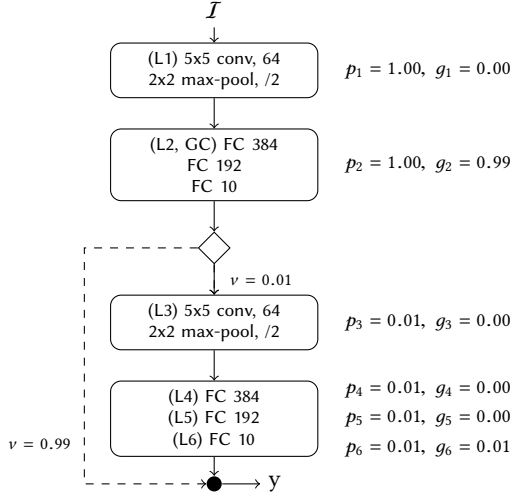
described in Figure 1b. The methodology outcome is particularly interesting showing that the Gate-Classification layer, being particularly demanding in terms of memory, is assigned to the Odroid-C2 n_{04} unit. When enough confidence is achieved at the Gate-Classification layer (i.e., $j = 2$), the decision is directly sent from n_{04} to the sink f through n_{06} . Otherwise, the processing is forwarded from n_{04} to n_{01} to complete the processing up to n_{08} and the classification is finally transmitted to f .

5.3 The configuration with multiple CNNs

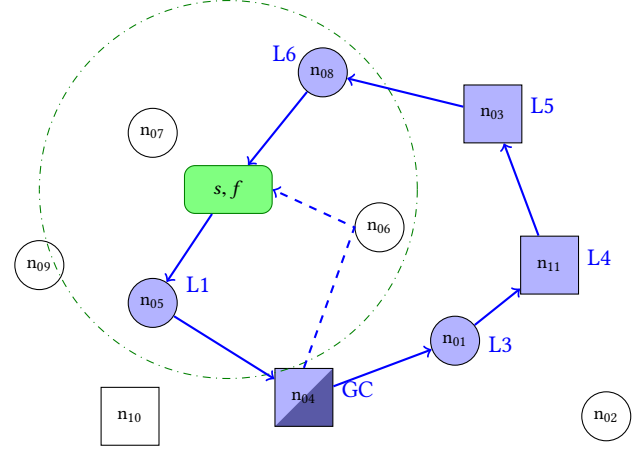
The methodology described in Section 4 is here tailored to the scenario where multiple CNNs (without and with shared processing layers) run in the same IoT system. We are not here considering Gate-Classification CNNs, hence all the layers are always executed leading to $p_{u,j}$ s equal to 1 (neglected in the formalization).

In this configuration, the objective function modelling the latency in decision making becomes:

$$\sum_{u=1}^C \sum_{i=1}^N \sum_{k=i}^N \sum_{j=1}^{M-1} \alpha_{u,i,j} \cdot \alpha_{u,k,j+1} \cdot \frac{K_{u,j}}{\rho} \cdot d_{i,k} + \sum_{i=1}^N t_i^{(p)} + t_s + t_f \quad (27)$$



(a) The architecture of the considered 6-layer Gate Classification CNN detailed in Table 1 along with the corresponding values of p_i and g_i , for each $i \in \mathbb{N}_N$. I is the input image.



(b) The outcome of the methodology applied on the 6-layer Gate-Classification CNN on the IoT system shown in Figure 1b. From the Gate-Classification layer (GC), the probability to take the dashed line path to n_{06} and the solid line path to n_{01} are 0.99 and 0.01, respectively. Note that the hop distance between the node n_{04} and the sink f is 2, thus n_{04} requires an intermediate hop, i.e., the node n_{06} , to send the final classification.

Figure 2: The configuration with a single Gate-Classification. The methodology is applied to the 6-layer Gate-Classification CNN shown in Figure 2a to the IoT system detailed in Figure 1b. The considered setting is $L = 1$.

with constraints defined in Eqs. (3), (4), (5) and (6), and where the source time t_s , the processing time $t_i^{(p)}$ and the sink time t_f are modified as follow:

$$t_s = \sum_{u=1}^C \sum_{i=1}^N \alpha_{u,i,1} \cdot \frac{K_{u,s}}{\rho} \cdot d_{s,i} \quad (28)$$

$$t_i^{(p)} = \sum_{u=1}^C \sum_{j=1}^M \alpha_{u,i,j} \cdot \frac{c_{u,j}}{e_i} \quad (29)$$

$$t_f = \sum_{u=1}^C \sum_{i=1}^N \alpha_{u,i,M_u} \cdot \frac{K_{u,M_u}}{\rho} \cdot d_{i,f} \quad (30)$$

At first, the proposed methodology has been applied to two instances of the 5-layer CNN described in Figure 1a without common processing layers, operating in the IoT system depicted in Figure 1b and with $L = 1$. The outcome of the methodology, depicted in Figure 3a, shows that the placement of both CNNs represent the optimal solution of the single-CNN configuration.

Moreover, the methodology has been applied to the case where the convolutional layers $L1$ and $L2$ are shared between the two CNNs. This solution is inspired by the transfer learning paradigm where two CNNs might share low-level representation processing layers, while high-level ones are specific for each CNN. As described in Section 4, the following constraints need to be added to the optimization problem:

$$\forall i \in \mathbb{N}_N \quad \alpha_{1,i,1} = \alpha_{2,i,1}, \quad (31)$$

$$\forall i \in \mathbb{N}_N \quad \alpha_{1,i,2} = \alpha_{2,i,2} \quad (32)$$

and the constraints Eq. (12), (13) and (14) to be redefined accordingly. The outcome of the methodology in this second scenario is particularly interesting showing that common layers $L1$ and $L2$ have been placed in IoT units n_{06} and n_{01} , respectively, while, after n_{01} the processing takes two different paths.

6 EXPERIMENTAL RESULTS

The proposed methodology has been validated on three state-of-the-art CNNs and two off-the-shelf IoT devices in a synthetic scenario of distributed image classification for the control a critical area (e.g., recognition of the presence of target objects in a given area through image classification).

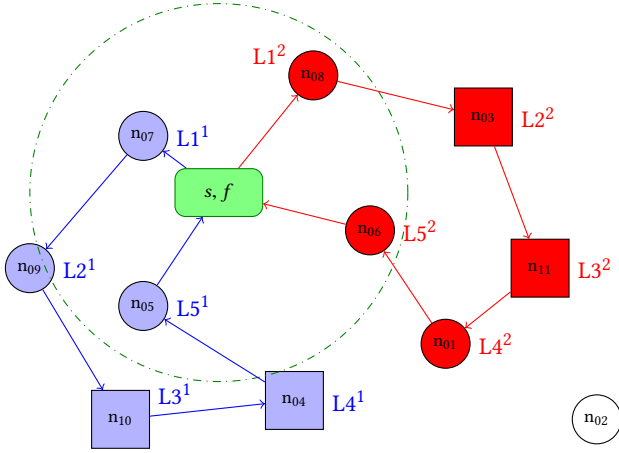
The monitored area is assumed to be a 30mx30m square and the positions of the IoT units as well as those of the sources s_u s and the sink f are randomly selected following a uniform distribution. The parameter L , setting the maximum number of CNN layers per IoT unit, ranges from 1 to 5.

The rest of the section is organized as follows. Section 6.1 details the considered CNNs, Section 6.2 describes the families of considered off-the-shelf IoT units, Section 6.3 presents the two considered transmission technologies, while Section 6.4 describes the figure of merit. Finally, Sections 6.5-6.6 describe the experimental results.

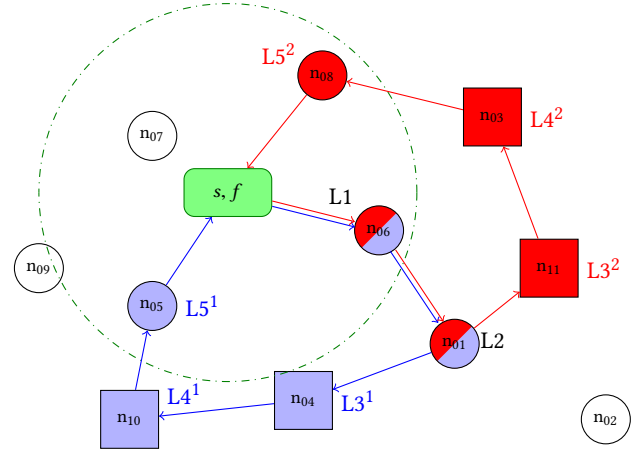
6.1 The considered CNNs

In the experimental section three state-of-the-art CNNs have been considered.

The first two CNNs are the 5-layer CNN shown in Figure 1a and the 6-layer Gate-Classification CNN shown in Figure 2a, respectively. These two CNNs, whose values of m_{js} , c_{js} , and K_{js}



(a) The outcome of the methodology when the two 5-layer CNNs are placed to the IoT system shown in Figure 1b. Here, no processing layer is shared between the CNNs and $L = 1$.



(b) The outcome of the methodology when the two 5-layer CNNs, sharing layer L1 and L2, are placed to the IoT system shown in Figure 1b. The setting is $L = 1$.

Figure 3: The multiple-CNN configuration. The methodology is here applied to two 5-layer CNNs detailed in Figure 1a on the IoT system shown in Figure 1b. We here considered the case where no processing layer is shared and the case where the first two layers, i.e., L1 and L2, are shared between the two CNNs.

are detailed in Table 1, receive in input a 28x28 RGB image and are composed by the following processing layers: a convolutional layer with 64 5x5 filters, a 2x2 maximum pooling with stride 2, a convolutional layer with 64 5x5 filters, a 2x2 maximum pooling with stride 2 and three fully-connected layers with 384, 192 and 10 neurons, respectively. In the 6-layer Gate-Classification CNN, the Gate-Classification layer is placed after the first pooling layer and is composed by three fully-connected layers with 384, 192 and 10 neurons, respectively.

The third CNN is the well-known AlexNet [18], whose details are given in Table 2. Such a CNN is endowed with 5 convolutional layers (with 96 11x11, 256 5x5, 384 3x3, 384 3x3 and 256 3x3 filters, respectively) and 3 fully-connected layers with 4096, 4096 and 2 neurons (as done in [11] to model a two-class problem). In addition, 3x3 maximum pooling layers with stride 2 are present after the first, second and fifth convolutional layers. A Gate-Classification variant of the AlexNet [11] has been considered where the Gate-Classifier is placed after the second maximum pooling layer and is composed of three fully-connected layers with 128, 64 and 2 neurons, respectively. Due to this complex architecture, the AlexNet has a higher demand in terms of memory and computational requirements than the other two CNNs.

In the four considered CNNs, the ReLUs, the batch normalization and the final softmax layers have not been explicitly mentioned since they have no parameter to store and negligible computation demands.

6.2 The considered IoT system

The considered IoT system comprises $N = 30$ IoT units belonging to two different technological families, i.e., the STM32H7 and the Raspberry Pi 3B+. The former refers to simple IoT units being endowed with a 400 MHz-Cortex M7 and 1 MB of RAM, while the

latter represents more powerful IoT units being endowed with a 1.4GHz 64-bit quad-core processor and 1GB of RAM. In the experiments we considered three different settings for the $N = 30$ IoT units partitioning: 10%-90%, 50%-50% and 90%-10%, where the first percentage refers to the probability of having a STM32H7 and the second one that of having a Raspberry Pi 3B+.

For both the STM32H7 and the Raspberry Pi 3B+, the maximum memory usage \bar{m}_i s has been defined as half of the available RAM memory, while the number of multiplications per second e_i s as a tenth of the clock cycles (per number of cores). The constraints on the computational load \bar{c}_i s have not been considered in this experimental section since they are application-specific. Details about \bar{m}_i s and e_i s are given in Table 3.

6.3 Transmission Technologies

The transmission technologies all the IoT nodes are equipped with are two, modelling two different scenarios:

- *high-bandwidth*, where the employed transmission technology is the *Wi-Fi 4* (standard IEEE 802.11n). The transmission range has been set to a tenth of the minimum indoor range, i.e., $d_t = 7.5m$, whereas the data-rate is $\rho = 72.2$ Mb/s, that corresponds to the single-antenna scenario with 64-QAM modulation on the 20 MHz channel, according to the specifications [22].
- *low-bandwidth* (and energy-consumption), where the *Wi-Fi HaLow* (standard IEEE 802.11ah), specifically designed for IoT systems, is adopted. The transmission range is equal to the other scenario, while the data-rate is $\rho = 7.2$ Mb/s with a single-antenna and 64-QAM modulation on the 2 MHz channel [1].

Table 1: The memory demand m_j , the computational load c_j , and the memory K_j required to store the intermediate representations of the 5-layer CNN and the 6-layer Gate-Classification CNN described in Section 5, where the Gate-Classification layer is marked with an asterisk. For the Gate-Classification the value K_j indicates the dimensions of the representation sent to the layer $j + 1$ when the classification is not taken at layer j . The memory requirements m_j and the image representations K_j are expressed in KB by using a 4B data type to store the representation, whereas the computation load c_j is in million (10^9) of multiplications.

Layer (j)		m_j	c_j	K_j
s	Source	-	-	9.41
1 ₁	5x5 conv, 64	19.20	3.76	200.70
1 ₂	2x2 pool, /2	-	0.05	50.18
2*	gc1 (fc 384,192,10)	19 570.18	4.89	50.18
3 ₁	5x5 conv, 64	409.60	20.07	50.18
3 ₂	2x2 pool, /2	-	0.01	12.54
4	fc 384	4 816.90	1.20	1.54
5	fc 192	294.91	0.07	0.77
6	fc 10	7.68	$2 \cdot 10^{-3}$	0.04

6.4 Figures of merit

The proposed methodology is evaluated on the “data production to decision making”-latency t defined as the time between the acquisition of the image and the reception of the classification outcome. To further clarify the effects of transmission and computation, latency t is split into the transmission t_t and the processing t_p terms. The former measures all the transmissions (from a source to IoT units, between IoT units, or from IoT units to the target unit f); the latter measures the processing time on each IoT unit. These terms are computed as defined in Section 4, whereas additional sources of delays, such as transmission handshakes or repeated transmissions due to failures have been neglected.

For each setting, transmission technology, and configuration, the evaluated metric is the mean \pm standard deviation of each latency term, i.e., t , t_t , and t_p , computed on 1000 randomly generated IoT systems.

6.5 The multi-CNN configuration

In this configuration, two 5-layer CNNs have to be placed on the IoT system detailed in Section 6.2 both with and without the first two (convolutional) layers shared. Moreover, the case associated to the maximum value of L (here 5) refers to the case where the whole computation can be executed on a single node⁵. This case can be seen as an approximation of sending data directly to the Cloud and then receiving back the result.

Results are presented in Table 4, for all the three configurations and the two transmission technologies. Several comments can be

⁵When the first two layers are shared this assumption cannot be made since it is reasonable to assume that the optimal solution will have a CNN entirely placed on a node n_1 , whereas the second has the first two layers on n_1 and the remaining ones on another node.

Table 2: The memory demand m_j , the computational load c_j , and the memory K_j required to store the intermediate representations of the AlexNet [18] and of its Gate-Classification version, where the Gate-Classification layer is marked with an asterisk, both adapted to a 2-class problem as in [11]. For the Gate-Classification the value K_j indicates the dimensions of the representation sent to the layer $j + 1$ when the classification is not taken at layer j . The memory requirements m_j and the representation cardinalities K_j are expressed in KB by using a 4B data type to store the representation, whereas the computation requirements c_j in million (10^9) of multiplications.

Layer (j)		m_j	c_j	K_j
s	Source	-	-	618.35
1 ₁	11x11 conv, 96, /4	139.78	105.42	1161.60
1 ₂	3x3 pool, /2	-	0.31	279.94
2 ₁	5x5 conv, 256	1 229.82	223.95	746.50
2 ₂	3x3 pool, /2	-	0.39	173.06
3*	gc1(fc 128,64,2)	22185.22	5.55	173.06
4	3x3 conv, 384	3 540.48	149.52	259.58
5	3x3 conv, 384	2 655.74	112.14	259.58
6 ₁	3x3 conv, 256	1 770.50	74.76	173.06
6 ₂	3x3 pool, /2	-	0.08	36.86
7	fc 4096	151 011.39	37.75	16.38
8	fc 4096, 2	67 158.02	16.78	16.38

Table 3: The maximum memory usage \bar{m}_i (defined as a half of the available RAM), and the number of multiplications per second e_i s (defined as a tenth of the clock cycles performed in one second) of three off-the-shelf IoT units.

Node (i)		\bar{m}_i	e_i
S1	STM32H7	512 KB	40
R1	Raspberry Pi 3B+	512 MB	560
O1	Odroid-C2	1 GB	600

made. At first, in the configurations with 90%-10% as partition between STM32H7 and Raspberry, the methodology has to often rely on STM32H7 nodes, then significantly increasing the processing time (the computation capability e of a Raspberry is 14 times greater than that of a STM32H7). However, it is possible to observe that the latency t is only 2 to 4 times greater than that of other configurations (except for $L = 1$ with Wi-Fi 4). This result is even more evident when some layers are shared, since the methodology can place less computation on STM32H7s. In general, the case with two shared layers is almost comparable to the case with no shared layers, independently from the considered configuration.

After that, the Wi-Fi 4 technology guarantees transmission latencies negligible w.r.t. the processing time, which represents more than 85% of latency t (96-99% with $L > 2$). Interestingly, the processing time is always equal to 89.9 ms, representing the experimental

Table 4: The multi CNN configuration results with $N = 30$ STM32H7 and Raspberry Pi 3B+ units and two 5-layer CNNs, in the three scenarios. The figures of merit, over 1000 experiments, are the latency t and its two components, i.e., the transmission time t_t and the processing time t_p . The proposed values are the sum over all the CNNs and are expressed in milliseconds.

(a) The results with the Wi-Fi 4 as adopted transmission technology. The three main-columns represent the results corresponding to the three scenarios, denoted as the percentage distribution of the STM32H7 and the Raspberry 3B+. All the values are expressed in milliseconds.

		10-90			50-50			90-10		
	L	t_t	t_p	$t = t_t + t_p$	t_t	t_p	$t = t_t + t_p$	t_t	t_p	$t = t_t + t_p$
No shared layers	1	14.7 ± 0.3	89.9 ± 0.0	104.6 ± 0.3	15.6 ± 1.1	89.9 ± 0.1	105.4 ± 1.1	19.4 ± 5.5	634.4 ± 417.0	653.8 ± 413.6
	2	3.4 ± 0.1	89.9 ± 0.0	93.3 ± 0.1	3.8 ± 0.6	89.9 ± 0.0	93.6 ± 0.6	10.2 ± 5.0	317.1 ± 401.5	327.3 ± 399.7
	3	0.9 ± 0.1	89.9 ± 0.0	90.7 ± 0.1	1.1 ± 0.4	89.9 ± 0.0	90.9 ± 0.4	4.0 ± 2.9	198.0 ± 240.0	201.9 ± 242.4
	4	0.7 ± 0.1	89.9 ± 0.0	90.6 ± 0.1	0.8 ± 0.3	89.9 ± 0.0	90.7 ± 0.3	4.0 ± 4.5	119.8 ± 67.0	123.7 ± 71.2
	5	0.5 ± 0.1	89.9 ± 0.0	90.4 ± 0.1	0.7 ± 0.3	89.9 ± 0.0	90.5 ± 0.3	3.0 ± 2.8	105.1 ± 34.1	108.1 ± 36.6
First two layers shared	1	14.6 ± 0.1	89.9 ± 0.0	104.5 ± 0.1	15.4 ± 1.2	89.9 ± 0.1	105.3 ± 1.2	23.4 ± 9.0	452.8 ± 470.8	476.2 ± 467.4
	2	3.4 ± 0.1	89.9 ± 0.0	93.3 ± 0.1	3.7 ± 0.5	89.9 ± 0.0	93.5 ± 0.5	9.6 ± 8.6	250.6 ± 389.8	260.2 ± 388.0
	3	2.0 ± 0.0	89.9 ± 0.0	91.9 ± 0.0	2.2 ± 0.4	89.9 ± 0.0	92.1 ± 0.4	7.1 ± 5.2	115.9 ± 63.1	122.9 ± 65.8
	4	0.8 ± 0.0	89.9 ± 0.0	90.7 ± 0.0	0.9 ± 0.3	89.9 ± 0.0	90.8 ± 0.3	2.3 ± 1.6	90.5 ± 1.3	92.8 ± 2.2
	5	0.8 ± 0.0	89.9 ± 0.0	90.6 ± 0.0	0.8 ± 0.2	89.9 ± 0.0	90.7 ± 0.2	2.0 ± 1.4	90.2 ± 0.6	92.2 ± 1.7

(b) The results with the Wi-Fi HaLow as adopted transmission technology. The three main-columns represent the results corresponding to the three scenarios, denoted as the percentage distribution of the STM32H7 and the Raspberry 3B+. All the values are expressed in milliseconds.

		10-90			50-50			90-10		
	L	t_t	t_p	$t = t_t + t_p$	t_t	t_p	$t = t_t + t_p$	t_t	t_p	$t = t_t + t_p$
No shared layers	1	147.2 ± 2.3	89.9 ± 0.3	237.2 ± 2.3	154.4 ± 11.5	91.2 ± 6.1	245.6 ± 14.1	187.0 ± 41.4	624.6 ± 416.9	811.6 ± 394.1
	2	34.5 ± 1.5	89.9 ± 0.0	124.4 ± 1.5	37.4 ± 5.3	90.0 ± 0.6	127.4 ± 5.4	95.3 ± 44.4	301.7 ± 383.1	397.0 ± 372.3
	3	8.8 ± 1.2	89.9 ± 0.3	98.8 ± 1.3	9.9 ± 2.7	90.4 ± 0.9	100.3 ± 3.0	32.9 ± 28.8	188.1 ± 228.8	221.0 ± 254.2
	4	7.0 ± 1.0	89.9 ± 0.0	96.9 ± 1.0	8.1 ± 2.6	89.9 ± 0.0	98.0 ± 2.6	37.5 ± 42.6	116.6 ± 64.0	154.1 ± 105.1
	5	5.3 ± 0.9	89.9 ± 0.0	95.2 ± 0.9	6.4 ± 2.7	89.9 ± 0.0	96.3 ± 2.7	28.6 ± 27.0	103.5 ± 32.6	132.1 ± 57.2
First two layers shared	1	146.6 ± 1.6	89.9 ± 0.3	236.5 ± 1.7	152.3 ± 9.8	90.7 ± 1.2	243.1 ± 10.1	223.7 ± 63.6	454.4 ± 459.1	678.0 ± 434.8
	2	34.1 ± 0.7	89.9 ± 0.2	124.0 ± 0.8	36.0 ± 4.3	90.2 ± 0.9	126.2 ± 4.5	85.4 ± 72.2	252.5 ± 389.8	338.0 ± 381.7
	3	20.4 ± 0.7	89.9 ± 0.2	110.3 ± 0.7	21.9 ± 3.9	90.1 ± 0.6	112.1 ± 4.0	65.3 ± 46.3	117.0 ± 62.8	182.3 ± 97.5
	4	8.4 ± 0.3	89.9 ± 0.2	98.3 ± 0.4	9.0 ± 2.2	90.2 ± 0.9	99.2 ± 2.4	17.9 ± 14.1	92.1 ± 1.5	110.0 ± 14.4
	5	7.6 ± 0.3	89.9 ± 0.2	97.5 ± 0.3	8.2 ± 2.2	90.0 ± 0.5	98.2 ± 2.2	17.1 ± 14.1	91.0 ± 0.7	108.0 ± 14.2

minimum achievable value in this IoT system. This consideration is no longer valid with the Wi-Fi HaLow, where the two terms are comparable, especially when $L = 1$. In particular, in the configurations with the 90% of Raspberry, the processing time can be slightly greater than 89.9 ms, involving in the computation also near STM32H7 nodes.

Finally, in all the cases with $L \geq 3$ (and $L = 2$ with Wi-Fi 4), the total latency t is comparable to the case ($L = 5$) where all the computation is expected to be placed on a single node. It is crucial to point out the importance of this result, because distributing the CNNs processing on various IoT nodes with a negligible increment in latency t will allow to define a pipeline in processing a sequence of images. Indeed, when a node has carried out its computation about an image or on one its intermediate representation (i.e., it has completed the processing of CNN layers is designed to), and sent the computed representation to the subsequent node, it is ready to operate on the next image, as in microprocessor pipelines. Hence, the throughput of CNN processing can be significantly increased

by processing images in pipeline, thus without waiting for the final classification. The bottleneck then becomes the IoT unit responsible for the highest processing time.

6.6 The configuration with a single (Gate-Classification) CNN

This configuration encompasses a single source and a single CNN (detailed in Tables 1 and 2), either with or without a Gate-Classifier, to be placed on the IoT system described in Section 6.2. The methodology is tested with the number of layers per node L ranging between 1 and 4, and compared to the situation where all the layers can be placed on the same node as done in Section 6.5 (in the results this case is indicated as $L = C$).

The results are shown in Table 5, for both transmission technologies in the partition setting 50%-50%. Interesting results arise. First of all, the expected processing time t_p is significantly reduced when the Gate-Classification is employed, as expected and studied in [11] for both the considered CNNs. In the case of 5-layer CNN,

Table 5: The single source single CNN configuration results with $N = 30$ STM32H7 and Raspberry Pi 3B+ units in the 50%-50% scenario, where each CNN is considered both with and without the Gate-Classifier (please refer to Tables 1 and 2 for details). The figures of merit, over 1000 experiments, are the latency t and its two components, i.e., the transmission time t_t and the processing time t_p . The proposed values are expressed in milliseconds.

CNN	L	Wi-Fi 4			Wi-Fi HaLow		
		t_t	t_p	$t = t_t + t_p$	t_t	t_p	$t = t_t + t_p$
5-layer CNN	1	7.49 ± 0.36	44.93 ± 0.00	52.42 ± 0.36	74.82 ± 3.94	45.16 ± 0.57	119.98 ± 4.06
	2	1.78 ± 0.21	44.93 ± 0.00	46.71 ± 0.21	17.75 ± 2.08	44.93 ± 0.00	62.68 ± 2.08
	3	0.48 ± 0.14	44.93 ± 0.00	45.41 ± 0.14	4.49 ± 0.89	45.08 ± 0.46	49.57 ± 1.03
	4	0.37 ± 0.11	44.93 ± 0.00	45.30 ± 0.11	3.64 ± 0.87	44.93 ± 0.00	48.57 ± 0.87
	C	0.28 ± 0.11	44.93 ± 0.00	45.21 ± 0.11	2.80 ± 0.88	44.93 ± 0.00	47.73 ± 0.88
6-layer GC CNN	1	5.87 ± 0.27	7.27 ± 0.00	13.14 ± 0.27	58.72 ± 2.47	7.27 ± 0.01	65.99 ± 2.47
	2	0.34 ± 0.10	7.27 ± 0.00	7.61 ± 0.10	3.53 ± 1.15	7.27 ± 0.00	10.80 ± 1.15
	3	0.29 ± 0.10	7.27 ± 0.00	7.57 ± 0.10	3.04 ± 1.10	7.27 ± 0.00	10.31 ± 1.10
	4	0.28 ± 0.10	7.27 ± 0.00	7.55 ± 0.10	2.90 ± 1.10	7.27 ± 0.00	10.17 ± 1.10
	C	0.28 ± 0.10	7.27 ± 0.00	7.55 ± 0.10	2.88 ± 1.10	7.27 ± 0.00	10.16 ± 1.10
AlexNet	1	203.06 ± 36.85	1257.71 ± 0.00	1460.77 ± 36.85	2042.48 ± 401.64	1265.89 ± 141.47	3308.37 ± 432.91
	2	127.81 ± 28.49	1257.71 ± 0.00	1385.52 ± 28.49	1298.23 ± 332.66	1263.16 ± 115.58	2561.39 ± 361.81
	3	98.75 ± 26.63	1257.71 ± 0.00	1356.46 ± 26.63	1009.79 ± 334.87	1260.44 ± 81.77	2270.22 ± 351.10
	4	95.82 ± 26.54	1257.71 ± 0.00	1353.53 ± 26.54	976.71 ± 317.48	1263.16 ± 115.58	2239.87 ± 348.56
	C	72.49 ± 24.08	1257.71 ± 0.00	1330.20 ± 24.08	750.02 ± 322.44	1260.44 ± 81.77	2010.46 ± 339.52
GC AlexNet	1	129.42 ± 28.29	598.92 ± 81.81	728.35 ± 86.17	1304.74 ± 310.87	598.93 ± 81.91	1903.66 ± 324.56
	2	93.70 ± 24.49	596.19 ± 0.00	689.89 ± 24.49	947.04 ± 258.12	596.19 ± 0.00	1543.23 ± 258.12
	3	72.10 ± 22.08	596.19 ± 0.00	668.29 ± 22.08	728.19 ± 221.12	596.19 ± 0.00	1324.38 ± 221.12
	4	72.07 ± 22.08	596.19 ± 0.00	668.26 ± 22.08	727.87 ± 221.10	596.19 ± 0.00	1324.06 ± 221.10
	C	71.84 ± 22.07	596.19 ± 0.00	668.03 ± 22.07	725.53 ± 220.95	596.19 ± 0.00	1321.72 ± 220.95

the Gate-Classification allows to save about 75-84% of the latency t , whereas on the AlexNet such gain is smaller but still significant (in the order of 34-50%)⁶.

After that, similarly to the multi-CNN case, when the Wi-Fi 4 is used, the transmission time t_p is significantly lower than the processing one t_p , thus it is reasonable to assume that the achieved t_p is the minimum feasible in this IoT system, corresponding to executing the CNN layers only on the most powerful available IoT units (i.e., the Raspberry 3B+). Moreover, when using the Wi-Fi HaLow, despite the transmission time t_t is comparable with the processing one t_p , the observed values of t_p are closer to the minimum achievable value, indicating that the methodology is still able to optimally place the CNN computation, relying on slower STM32H7 only when there is no alternative.

The third crucial comment is about the $L = C$ case. The latency t of this case and those of corresponding ones having $L > 2$ ($L > 3$ with Wi-Fi HaLow) are almost equal, showing the capability of the proposed methodology of distributing the CNN computation among nodes with negligible latency increments w.r.t. not distributing at all. Moreover, similarly to what commented in Section 6.5, the latency with $L = 1$ is comparable to case $L = C$, with an increment

smaller than 10% with Wi-Fi 4, but we can define a processing pipeline working on more than an image at a time: when a IoT unit has carried out of its assigned layers it is ready to process the next image.

7 CONCLUSIONS

The aim of this paper was to match deep learning solutions, which usually require high memory and computational demands, with IoT systems, whose units are generally constrained in memory and computation. To achieve this goal, deep learning solutions must be completely rethought to match the constraints characterizing IoT units. For the first time in the literature, this paper introduces a methodology for the design of Convolutional Neural Networks able to operate in IoT systems. The methodology has been formalized as an optimization problem, where the latency between image acquisitions and the decision making is minimized. The proposed methodology is general enough to be applied to multiple sources of data and multiple CNNs operating in the same IoT system.

Future works will encompass the extension of the methodology to manage failures or retransmissions in the communication. Moreover, the methodology could be extended to deal with mobile units as well as novel families of distributed computing paradigm such as Fog and Edge computing. To enable efficient re-distribution of the CNN processing among nodes in this scenario, where the nodes

⁶The latency t and its terms, i.e., t_t and t_p , are defined as an expected value when the Gate-Classification is involved, by weighting their values up to each layer j of CNN u with the probability $g_{u,j}$ of providing the final classification at that layer.

might join or leave the IoT system, an analysis of the optimization problem is required to design an algorithm to solve it with specific time guarantees. Similarly, an interesting aspect to be investigated in future works is the definition of a computational pipeline, similarly to those of CPUs, to process more images at the same time on the different involved IoT units, by defining the bottleneck and the gain of this approach.

REFERENCES

- [1] Toni Adame, Albert Bel, Boris Bellalta, Jaume Barcelo, and Miquel Oliver. 2014. IEEE 802.11 AH: the WiFi approach for M2M communications. *IEEE Wireless Communications* 21, 6 (2014), 144–152.
- [2] Md Golam Rabiul Alam, Yan Kyaw Tun, and Choong Seon Hong. 2016. Multi-agent and reinforcement learning based code offloading in mobile fog. In *Information Networking (ICOIN), 2016 International Conference on*. 285–290.
- [3] Cesare Alippi, Simone Disabato, and Manuel Roveri. 2018. Moving Convolutional Neural Networks to Embedded Systems: The AlexNet and VGG-16 Case. In *2018 17th ACM/IEEE International Conference on Information Processing in Sensor Networks (IPSN)*. IEEE, Porto, 212–223.
- [4] Cesare Alippi and Manuel Roveri. 2017. The (Not) Far-Away Path to Smart Cyber-Physical Systems: An Information-Centric Framework. *Computer* 50, 4 (apr 2017), 38–47.
- [5] Renzo Andri, Lukas Cavigelli, Davide Rossi, and Luca Benini. 2016. YodaNN: An ultra-low power convolutional neural network accelerator based on binary weights. In *2016 IEEE Computer Society Annual Symposium on VLSI (ISVLSI)*. IEEE, 236–241.
- [6] Itamar Arel, Derek C Rose, Thomas P Karnowski, et al. 2010. Deep machine learning—a new frontier in artificial intelligence research. *IEEE computational intelligence magazine* 5, 4 (2010), 13–18.
- [7] Florian Berg, Frank Dürr, and Kurt Rothermel. 2014. Optimal Predictive Code Offloading. In *Proceedings of the 11th International Conference on Mobile and Ubiquitous Systems: Computing, Networking and Services (MOBIQUITOUS '14)*. ICST (Institute for Computer Sciences, Social-Informatics and Telecommunications Engineering), ICST, Brussels, Belgium, Belgium, 1–10.
- [8] Lukas Cavigelli and Luca Benini. 2017. Origami: A 803-gop/s/w convolutional network accelerator. *IEEE Transactions on Circuits and Systems for Video Technology* 27, 11 (2017), 2461–2475.
- [9] Zixue Cheng, Peng Li, Junbo Wang, and Song Guo. 2015. Just-in-time code offloading for wearable computing. *IEEE Transactions on Emerging Topics in Computing* 3, 1 (2015), 74–83.
- [10] Emily L Denton, Wojciech Zaremba, Joan Bruna, Yann LeCun, and Rob Fergus. 2014. Exploiting linear structure within convolutional networks for efficient evaluation. In *Advances in Neural Information Processing Systems*. 1269–1277.
- [11] Simone Disabato and Manuel Roveri. 2018. Reducing the Computation Load of Convolutional Neural Networks through Gate Classification. In *2018 International Joint Conference on Neural Networks (IJCNN)*, Vol. 2018-July. IEEE, 208–215.
- [12] Song Han, Huizi Mao, and William J Dally. 2015. Deep compression: Compressing deep neural networks with pruning, trained quantization and Huffman coding. *arXiv preprint arXiv:1510.00149* (2015).
- [13] Kaiming He, Xiangyu Zhang, Shaoqing Ren, and Jian Sun. 2016. Deep Residual Learning for Image Recognition. In *The IEEE Conference on Computer Vision and Pattern Recognition (CVPR)*.
- [14] Robert D. Hof. 2013. 10 Breakthrough Technologies 2013: Deep Learning. *MIT Technology Review* (2013).
- [15] Kirak Hong, David Lillethun, Umakishore Ramachandran, Beate Ottenwälder, and Boris Koldehofe. 2013. Mobile Fog: A Programming Model for Large-scale Applications on the Internet of Things. In *Proceedings of the Second ACM SIGCOMM Workshop on Mobile Cloud Computing (MCC '13)*. ACM, New York, NY, USA, 15–20.
- [16] Richard M Karp. 1972. Reducibility among combinatorial problems. In *Complexity of computer computations*. Springer, 85–103.
- [17] L. Krishnamachari, D. Estrin, and S. Wicker. 2002. The impact of data aggregation in wireless sensor networks. In *Proceedings 22nd International Conference on Distributed Computing Systems Workshops*. 575–578.
- [18] Alex Krizhevsky, Ilya Sutskever, and Geoffrey E. Hinton. 2012. ImageNet classification with deep convolutional neural networks. In *Proceedings of the 25th International Conference on Neural Information Processing Systems - Volume 1 (NIPS '12)*, Vol. 1. Curran Associates Inc., 1097–1105.
- [19] Joseph Redmon, Santosh Divvala, Ross Girshick, and Ali Farhadi. 2016. You Only Look Once: Unified, Real-Time Object Detection. In *2016 IEEE Conference on Computer Vision and Pattern Recognition (CVPR) (CVPR '16)*. IEEE, 779–788.
- [20] Cong Shi, Vasileios Lakafofis, Mostafa H. Ammar, and Ellen W. Zegura. 2012. Serendipity: Enabling Remote Computing Among Intermittently Connected Mobile Devices. In *Proceedings of the Thirteenth ACM International Symposium on Mobile Ad Hoc Networking and Computing (MobiHoc '12)*. ACM, New York, NY, USA, 145–154.
- [21] Surat Teerapittayanon, Bradley McDanel, and Hsiang-Tsung Kung. 2017. Distributed deep neural networks over the cloud, the edge and end devices. In *2017 IEEE 37th International Conference on Distributed Computing Systems (ICDCS)*. IEEE, 328–339.
- [22] Yang Xiao. 2005. IEEE 802.11 n: enhancements for higher throughput in wireless LANs. *IEEE Wireless Communications* 12, 6 (2005), 82–91.
- [23] Jason Yosinski, Jeff Clune, Yoshua Bengio, and Hod Lipson. 2014. How transferable are features in deep neural networks?. In *Advances in neural information processing systems*. 3320–3328.